



## Release of TiO<sub>2</sub> – (Nano) particles from construction and demolition landfills



Ralf Kaegi<sup>a,\*</sup>, Alexander Englert<sup>b</sup>, Andreas Gondikas<sup>c,d</sup>, Brian Sinnet<sup>a</sup>, Frank von der Kammer<sup>d</sup>, Michael Burkhardt<sup>b</sup>

<sup>a</sup> Eawag, Swiss Federal Institute of Aquatic Science and Technology, Überlandstr. 133, 8609 Dübendorf, Switzerland

<sup>b</sup> HSR University of Applied Sciences, Institute of Environmental and Process Engineering (UMTEC), Oberseestrasse 10, 8640 Rapperswil, Switzerland

<sup>c</sup> University of Gothenburg, Department of Marine Sciences, Kristineberg 566, 45178 Fiskebäckskil, Sweden

<sup>d</sup> University of Vienna, Department of Environmental Geosciences, Althanstr. 14, UZA II, 1090 Vienna, Austria

### ARTICLE INFO

#### Keywords:

TiO<sub>2</sub> – particles  
Landfills  
White pigments  
Construction materials

### ABSTRACT

A large fraction of engineered nanomaterials (ENM) will be deposited in landfills and it is assumed that ENM are securely locked in landfill sites and cannot leach into the environment (e.g. surface waters). However, experimental evidence supporting this assumption is lacking, as current production volumes of ENM are still too small and/or analytical techniques not sensitive enough to allow for the detection and quantification of ENM in landfill leachates. TiO<sub>2</sub> particles are currently used in large quantities, for example in construction materials such as paints and renders as white pigments and their sizes extend into the nano-size range. We, therefore, selected TiO<sub>2</sub> particles as a surrogate to assess the potential release of ENM from construction and demolition (C & D) landfill sites. We collected leachate samples from a landfill over one year and used complementary analytical techniques, including inductively coupled plasma (ICP) – optical emission spectroscopy (OES), automated scanning electron microscopy (auto SEM), transmission electron microscopy (TEM) and single particle ICP - mass spectrometry (spICPMS) to quantify TiO<sub>2</sub> particles in landfill leachates. Total elemental Ti contents were mostly around a few tens of µg L<sup>-1</sup> and were strongly correlated with total suspended solids. Based on the volumetric discharge of the landfill leachate water from the landfill, we estimate a total amount of ~0.5 kg of TiO<sub>2</sub> particles that are released annually from the landfill. Ti concentrations derived from ICP-OES measurements were in good agreement with quantifications based on TiO<sub>2</sub> particles detected by auto SEM analyses. spICPMS measurements indicated a number concentration of Ti-containing particles in the order of 10<sup>5</sup> mL<sup>-1</sup> and TEM analyses dominantly revealed nanoscale TiO<sub>2</sub> particles with a spherical shape typically observed for TiO<sub>2</sub> particles used as white pigments. In addition, angular TiO<sub>2</sub> particles with a well-defined crystal habitus were detected, suggesting that also natural TiO<sub>2</sub> particles of comparable sizes are present in the landfill leachates.

The results from this study indicate that (nanoscale) TiO<sub>2</sub> particles are released from C & D landfill sites (~5 g/year). Although the amount of TiO<sub>2</sub> particles released from C & D landfill sites may still be rather low, these particles may serve as proxy for assessing the future release of ENM from C & D landfill sites, which may become relevant as an increasing use of ENM is predicted for construction materials in general.

### 1. Introduction

Engineered nanomaterials (ENM), such as SiO<sub>2</sub>-, TiO<sub>2</sub>- and Ag-nanoparticles (NP), are used in many consumer products to increase the performance of the respective goods, e.g. antimicrobial properties of textiles or scratch resistance of renders. However, these benefits have to be balanced against possible adverse effects of ENM when released in an uncontrolled way into the (aquatic) environment. Most of the currently available research on pathways of nanomaterials into the (aqueous) environment has been focused on the release from products during the use phase of the respective materials. For example, the

release of Ag-NP, TiO<sub>2</sub>-NP and SiO<sub>2</sub>-NP from outdoor paints, coatings and sunscreen has been addressed both under real-world (Kaegi et al., 2010; Kaegi et al., 2008; Gondikas et al., 2014) and laboratory conditions (Al-Kattan et al., 2013; Al-Kattan et al., 2014; Al-Kattan et al., 2015; Olabarrieta et al., 2012; Zuin et al., 2013; Zuin et al., 2014). Results from mass flow models (Keller et al., 2013; Sun et al., 2014; Gottschalk et al., 2009) suggest that the majority of ENM are deposited in landfills, and the importance to assess ENM release from solid waste in general has been well recognized (Boldrin et al., 2014; Marcoux et al., 2013; Reinhart et al., 2010; Bystrzejewska-Piotrowska et al., 2009).

\* Corresponding author.

E-mail address: [ralf.kaegi@eawag.ch](mailto:ralf.kaegi@eawag.ch) (R. Kaegi).

<http://dx.doi.org/10.1016/j.impact.2017.07.004>

Received 19 May 2017; Received in revised form 20 July 2017; Accepted 21 July 2017

Available online 15 August 2017

2452-0748/ © 2017 Elsevier B.V. All rights reserved.

The application of ENM in construction materials is of high interest as it may substantially increase the life time of construction materials and thus save on resources (Andresen et al., 2014). A substantial amount (~25%) of the nano-TiO<sub>2</sub> entering the waste management systems in Switzerland mainly results from the construction sector and is directly deposited in landfills, dedicated for inert materials (Mueller et al., 2013). Based on a survey of the Swiss construction industry, Hincapié et al. (2015) reported that ENM (nano-TiO<sub>2</sub>, nano-SiO<sub>2</sub>, nano-ZnO, and nano-Ag) are mainly applied in paints and cement and also van Broekhuizen and van Broekhuizen (2009) concluded that coatings and paints are important products where ENM are already in use. Therefore, paints are and will be important products containing ENM and for Switzerland, it has been shown that the majority of the paints enter either the recycling system (~75%) or are directly disposed in landfills (~25%) (Hincapié et al., 2015). Furthermore, ~85% of the paint that enters the recycling system ends up in landfills, and 15% remains as impurities in the recycled fraction. Thus, life cycle analyses (LCA) of ENM containing paints and façade coatings are hampered by the lack of long term emission data of ENM from landfill sites (Hischier et al., 2015). The same arguments hold true for end-of-life implications of ENM containing products which to a large extent also are landfilled (Asmatulu et al., 2012). However, ENM enhanced construction materials are still niche products with limited market shares (van Broekhuizen et al., 2011), resulting in small quantities currently landfilled and consequently, low concentrations of ENM are expected in the respective landfill leachate. Due to the rather long lifetime of today's buildings ranging up to 80 years it may take decades before ENMs start flowing out to different compartments (Hincapié et al., 2015). This, in combination with the presence of natural nanoscale materials (e.g. nanoscale TiO<sub>2</sub>), possibly resulting from slightly contaminated soils which can also landfilled in C & D landfill sites, makes it very challenging to unambiguously identify ENM in landfill leachates.

Despite the importance of ENM in construction materials and their dominant flows into landfills, release of ENM from landfill sites have not been considered so far and landfill sites are commonly treated as final sinks for ENM (e.g. Sun et al. (2014), Mitrano et al. (2015)), although there are no experimental evidence to underline this claim. On the contrary, the release/export of pollutants (organic pollutants and heavy metals) from landfills sites has at least to some extent been explained by the colloidal – facilitated transport (Matura et al., 2012; Matura et al., 2010; Baumann et al., 2006). Jensen and Christensen (1999) investigated the metal loads of four different municipal solid waste landfills in Denmark and found a substantial fraction of the heavy metals such as Zn, Pb, and Cd in the lower colloidal size range (1 nm–400 nm). In another study, stable colloids in the 0.1–1 µm range were reported from municipal landfill leachates and it was suggested that a coating with organic macromolecules likely was responsible for the steric stabilization of the colloids (Gounaris et al., 1993). Interaction of spiked ENM (ZnO, Ag, TiO<sub>2</sub>) with matrix components of landfill leachates (e.g. Cl<sup>-</sup>, ammonia, humic acid) resulted in either dissolution or stabilization of the ENM in the leachate, but neither the aerobic (BOD<sub>5</sub>) nor anaerobic (biogenic methane production) processes were compromised by the addition of ENM to leachates (Bolyard et al., 2013). Enhanced colloidal stability resulting from a combination of electric and steric effects and consequently mobility of single-walled carbon nanotubes were observed in experimental landfill leachates in the presence of humic acid (Khan et al., 2013; Lozano and Berge, 2012). Efficient retention (mostly around 90%) of nano-TiO<sub>2</sub> spiked to real and synthetically prepared municipal solid waste under different conditions (variable pH and different ionic strengths) was observed during short term (3 days) batch experiments (Dulger et al., 2016). Although all components of the MSW contributed to the retention of the TiO<sub>2</sub> within the MSW matrix, this study suggests that (limited) leaching of nano TiO<sub>2</sub> from MSW is not unrealistic. Hennebert et al. (2013) detected various nanoscale colloids in a large set of experimentally leached waste materials. Based on stepwise filtration experiments conducted on

a limited number of leachates collected from landfills containing incineration residues, Mitrano et al. (2017) reported variable types of (nanoscale) colloids at different concentrations in the leachates. This short overview demonstrates that i) a significant fraction of ENM is and will be deposited in construction and demolition (C & D) landfills ii) colloids/ENM can be colloiddally stabilized and mobilized under landfill leachate conditions especially in the presence of organics (humic acid) and iii) field data on the release of ENM from real (C & D) landfills are entirely lacking. Thus, the goal of this study was to evaluate whether ENM can be released from C & D landfills and thus enter the surface waters. The use of ENM in construction materials is still in its infancy, but TiO<sub>2</sub> particles are used in construction materials since many decades, for example as white pigments, with a typically mean size of 250 to 450 nm (Hempelmann et al., 2005). These particles may thus not qualify as ENM in a strict sense, but also TiO<sub>2</sub> pigments have a considerable fraction based on the number size distribution that extends into the nanoscale (Kaegi et al., 2008; Weir et al., 2012). We, therefore, used TiO<sub>2</sub> particles already contained in the building materials as surrogate particles to assess future release pathways of ENM from landfilled C & D materials and thus to evaluate the relevance of C & D materials as potential sources for ENM release to surface waters.

## 2. Materials & methods

### 2.1. Landfill site and sample collection

In Switzerland, C & D landfills sites have to fulfill stringent criteria reading permeability of the underground (e.g. minimum of 2 m of geological barrier with an average hydraulic conductivity (k) of < 1.0 × 10<sup>-7</sup> ms<sup>-1</sup> in any direction or an engineered barrier of comparably quality) and drainage of the leachate to protect water resources (Der Schweizerische Bundesrat, 2011). The landfill studied in this project is located in the Northeastern part of Switzerland. It covers an area of roughly 30,000 m<sup>2</sup> and contains about 220,000 m<sup>3</sup> of inert waste, e.g. glass, pottery, soil excavation, concrete and mixed demolition materials. The regular operation started 2010. The leachate is collected in a central pipe and discharged into a separated stormwater system that discharges after 1 km into the river Rhine without any further treatment. More than 20 leachate samples were collected over the period of one year. Samples were collected in 3 × 1 L SCHOTT – glass bottles, which were rinsed 3 times with the leachates before the samples were collected. Temperature, pH, O<sub>2</sub> and electrical conductivity were measured onsite (WTW Multiline 3430, Xylem Analytics, Germany). The samples were immediately transported into the laboratory and processed for further analyses within < 3 h. Total suspended solids (TSS) were determined by filtering 1 L of leachate through glass microfiber filters (GF/F, 25 mm, diameter Whatman, GE Healthcare, USA) and drying the filter at 105 °C.

### 2.2. Elemental analyses

Total elemental contents of the particulate matter were determined using inductively coupled plasma – optical emission spectrometry (ICP-OES, CirusCCD, SPECTRO Analytical Instruments GmbH, Germany). In general, 1 L of landfill effluent was filtered through 0.2 µm cellulose acetate membrane filters (47 mm, Whatman, GE Healthcare, USA). The filter was digested in a mixture of HNO<sub>3</sub> (1 mL, 65%, ultrapure, Merck), HF (200 µL, 48%, Merck) and H<sub>2</sub>O<sub>2</sub> (200 µL, 35%, Merck) using a microwave assisted acid digestion system (UltraClave 3, MLS GmbH) and the clear digest was filled to 50 mL with doubly deionized (DDI) water. Instrumental detection limits for Ti were 1 µg L<sup>-1</sup> which translates into 0.05 µg L<sup>-1</sup> for the digested landfill samples as 1 L of sample was filtered and the digested filters were filled to 50 mL. Ti concentrations of digested filters (blanks) were below the detection limit.

### 2.3. Electron microscopy

#### 2.3.1. Scanning electron microscopy (SEM)

Particles with a diameter  $> 400$  nm were collected on Nuclepore filters (0.4  $\mu\text{m}$  pore diameter, 25 mm diameter, Whatman®, Nuclepore™ Track-Etched Membranes, GE Healthcare, USA) and investigated using an SEM (Nova NanoSEM230, FEI, USA) operated at an acceleration voltage of 15 kV. Depending on the TSS content, 1–5 mL of landfill leachate were filtered through the Nuclepore filters which we subsequently coated with a thin layer of carbon ( $\sim 10$  nm) using a carbon coater (ACE200, Leica Microsystems, Germany) to increase the electrical conductivity of the filter. For the automated SEM analyses, C-coated filters were put on 50 mm (diameter) Cu discs, having a central inset for a carbon disc (25 mm diameter). This carbon disc was used to avoid any Cu signal that would be generated when putting the filter directly on the Cu-disc. An additional Cu ring (inner diameter 20 mm) was used to fix the filter to the Cu disc. Individual particles were detected based on backscattered electron (BSE) images and the elemental composition of every particle (500 nm–10  $\mu\text{m}$ ) was determined by using an energy dispersive X-ray (EDX) system (INCA, Oxford Inst., UK). BSE imaging and EDX analysis of the detected particles was conducted using an automated particle analysis system (feature analysis included in the INCA software package, Oxford Inst., UK). In total, between 1700 and 3700 particles were detected per filter and 6 different filters were analyzed. Measurements were typically conducted over-night and lasted about 6 h. The parameters of all individual particles, including equivalent spherical diameter and elemental composition, were exported as text files and further processed using Matlab (R2012b). In addition to the  $\text{TiO}_2$ -polymorphs Rutile, Anatase and Brookite, major Ti bearing mineral phases are Ilmenite, Sphene and Perovskite (Deer et al., 1992). However, these minerals are neither expected to occur in constructions materials nor in the sedimentary rocks surrounding the landfill. A small fraction of Ti may also be associated with clay minerals. However, the Ti-contents of clay minerals generally do not exceed a few weight percent (wt%). Therefore, all particles with a Ti content  $> 20$  wt% were assigned to  $\text{TiO}_2$  particles. Between 11 and 48  $\text{TiO}_2$  particles were detected per filter, which was not enough to derive a particle size distribution (PSD). We assumed that the size distribution of the  $\text{TiO}_2$  particles was similar in all samples and we, therefore, combined  $\text{TiO}_2$  particles from all samples to derive a PSD for the  $\text{TiO}_2$  particles. To calculate the total Ti concentration from the number-based size distributions, the modeled PSD was scaled to the amount of particles detected on each filter and the mass of the individual particles was calculated assuming a spherical particle morphology and a density of  $4.24 \text{ g cm}^{-3}$ , corresponding to the density of rutile. Two samples were measured 3 times with the automated particle analysis system on different days. The calculated Ti concentrations were 6.7, 5.2 and  $7.6 \mu\text{g L}^{-1}$  and 30, 47 and  $38 \mu\text{g L}^{-1}$ , respectively.

#### 2.3.2. Transmission electron microscopy (TEM)

To detect nanoscale  $\text{TiO}_2$  particles, selected samples were analyzed using a scanning transmission electron microscope (STEM, HD-2700-Cs, Hitachi, Japan), operated at an acceleration voltage of 200 kV. Samples for STEM analyses were prepared by direct on-grid centrifugation (Mavrocordatos and Perret, 1995) using carbon coated copper grids (PlanoEM or Quantifoil, DE). To avoid overlapping of larger and smaller particles, and as the particles  $> 500$  nm were investigated using auto SEM, larger particles were removed from the suspension by centrifugation (5 min @ 700 rpm,  $\sim 60 \times g$ ). The supernatant (2 cm) was then removed and directly centrifuged on TEM grids (1 h @ 14,000 rpm,  $\sim 24,000 \times g$ ).

Images were recorded using either a bright field (BF) or a high-angular annular dark field (HAADF) detector. Elemental analysis of individual particles was performed using an energy dispersive X-ray detector (EDAX, USA) and the spectra were recorded and processed using Digital Micrograph (v.1.85, Gatan Inc., USA).

### 2.4. Single particle ICP-MS analyses

Collected landfill leachates were filtered (0.4  $\mu\text{m}$  pore diameter, 25 mm diameter, Whatman®, Nuclepore™ Track-Etched Membranes, GE Healthcare, USA) to remove larger particles, dispersed (two minutes sonication in a vial tweeter (Hielscher Ultrasonics GmbH, Germany)) and finally stabilized (addition of 0.1 wt% NovaChem 100 (mix of nonionic and ionic detergents for FFF applications, Postnova Analytics GmbH, Germany)). Treated samples were sent to the University of Vienna for spICPMS measurements (Agilent 8800, Santa Clara, CA, USA). To assess potential changes of the particles during sample transport, we measured the average diameter of the particles by dynamic light scattering (DLS, nanoZS, Malvern, UK). To avoid isobaric interferences of  $^{48}\text{Ti}$  with  $^{48}\text{Ca}$ ,  $\text{NH}_3$  was used as a reaction gas and Ti was detected at  $63 m/z$  as  $^{48}\text{Ti}^{14}\text{NH}^+$  (Tharaud et al., 2017). Gold nanoparticles (60 nm, NIST, RM8013) and dissolved Au standards (0, 0.025, 0.1, and  $1 \mu\text{g L}^{-1}$ ) and Ti standards (0, 25, 100, and  $1000 \mu\text{g L}^{-1}$ ) were used to determine the nebulization efficiency (6.4%) and to convert the Ti signal intensities into masses. For the calibration measurements we used a dwell time of 4 ms and the leachate samples were measured at a dwell time of 3 ms. The settling time was fixed to 0.5 ms in all measurements. Data analysis was conducted using the Nanocount software (Cornelis, 2014). The size detection limit, i.e. the lowest quantifiable particle diameter, assuming stoichiometric  $\text{TiO}_2$  was 110 nm. Recorded signal intensities were converted into particle size frequencies which were transformed into discrete particle number concentrations. Data from five blanks (MilliQ water) were processed the same way and the resulting, averaged particle size distribution (mostly false positives close to the size detection limit) served as a background and was subtracted from the particle size distribution obtained for the landfill samples.

## 3. Results and discussion

In the following discussion, we will refer to  $\text{TiO}_2$  particles, if the employed methods allow an unambiguous identification of the respective particles. If the methods do not allow distinguishing between pure  $\text{TiO}_2$  particles (consisting only of Ti and O) and other sources of particulate Ti (e.g. Ti in clay minerals), we will refer to as Ti-particles.

### 3.1. Physical and chemical properties of the leachates

The basic physical chemical parameters of the collected samples are summarized in Table 1. The sample Nr. 16 was collected shortly after an extreme rain event and showed very different characteristics (e.g.  $> 500 \text{ mg L}^{-1}$  TSS, pH = 5.2) compared to the other leachate samples. We, thus, assume this sample was strongly dominated by surface runoff from the nearby cropped soils and does not reflect typical landfill leachates. For that reason, this sample is excluded from the following analysis.

The temperature of the leachates varied between 12 and 14  $^\circ\text{C}$  and the  $\text{O}_2$  content was close to saturation ( $\sim 10 \text{ mg L}^{-1}$  at 13  $^\circ\text{C}$ ). The pH of the leachate was between 5.9 and 8.0. The TSS concentrations were between 2 and  $73 \mu\text{g L}^{-1}$  and the Ti concentration generally varied between 10 and  $170 \mu\text{g L}^{-1}$ . The volumetric discharge rate of the landfill varied between  $0.04 \text{ L s}^{-1}$  and  $2.5 \text{ L s}^{-1}$  (Fig. S1).

Both TSS - and Ti contents vary over more than one order of magnitude (Table 1), however, these two parameters show a strong positive correlation ( $R = 0.94$ , Fig. 1). This correlation indicates that Ti-particles are leached proportionally to the TSS content in the landfill leachate and TSS may be used to get a rough estimate about the Ti content in the leachate. The correlation between the Ti content and the recorded volumetric effluent flow rate, however, is rather poor ( $R = 0.55$ ,  $n = 12$ ) suggesting that the release of both Ti and TSS in general follows more complex patterns and cannot be predicted based on the volumetric flow rate.

**Table 1**  
Physical and chemical parameters of the landfill effluents.

Sample number	TSS (mg L <sup>-1</sup> )	pH	O <sub>2</sub> (mg L <sup>-1</sup> )	Conductivity (μS cm <sup>-1</sup> )	Temperature (°C)	Ti conc. (mg L <sup>-1</sup> ) <sup>b</sup>
1	18	8.0	10.0	1527	14.3	0.103
2	5.4	7.7	9.9	1865	13.7	0.026
3	16	7.6	9.3	2250	13.2	0.037
4	NA	7.8	9.9	2240	13.3	0.045
5	73	7.8	9.4	1803	13.6	0.167
6	6.0	7.8	9.4	2170	13.2	0.018
7	16	7.2	10.0	2130	13.2	0.029
8	3.2	7.4	9.9	2030	13.4	0.012
9	6.3	7.1	9.4	1948	13.5	0.022
10	3.2	6.8	9.3	1821	14.4	0.010
11	2.1	6.8	9.5	1735	14.0	0.008
12	2.9	7.0	10.0	2200	13.5	0.011
13	19	6.1	10.1	2170	11.9	0.056
14	8.1	5.9	10.9	1764	9.7	0.024
15	6.1	6.6	6.2	NA	12.0	0.015
16	560	5.2	9.2	16,634	13.4	3.739
17 <sup>a</sup>	7.4	7.7	9.8	1820	12.9	0.015
18 <sup>a</sup>	7.4	7.7	9.8	1820	12.9	0.022
19 <sup>c</sup>	5.9	7.7	9.5	1893	NA	0.018

NA: not available.

<sup>a</sup> Duplicates.

<sup>b</sup> Measured with ICP-OES.

<sup>c</sup> Additional spICPMS measurements conducted.

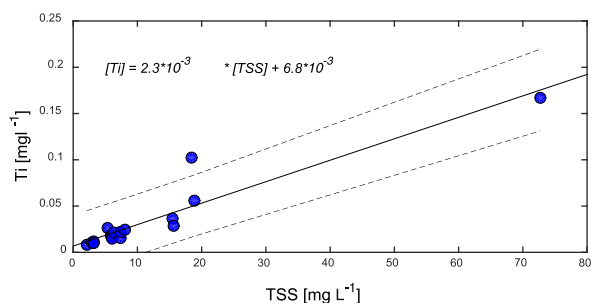


**Fig. 1.** Total Ti content (measured with ICP-OES) vs. TSS of landfill leachate samples. The solid line represents the best fit and the dashed line indicates the prediction intervals (95%).

Based on the average Ti concentrations (0.035 mg l<sup>-1</sup>) derived from ICP-OES measurements and in combination with recorded discharge volumes of the landfill site for the year 2014 (~8000 m<sup>3</sup>, Fig. S1), the annually discharged mass of Ti was ~0.3 kg. The bulk Ti concentrations provided initial evidence of the release of Ti-particles from the C&D landfill, but neither the size nor the elemental composition of individual particles can be extracted from total elemental concentrations. Therefore, we conducted electron microscopic analysis complemented by spICPMS measurements to identify individual TiO<sub>2</sub> particles and to determine their size distribution.

### 3.2. Release of TiO<sub>2</sub> – particles (500 nm–10 μm)

Particles with a diameter > 400 nm were collected on Nuclepore filters and investigated using auto SEM. The particle size distribution (PSD) including i) all particles and ii) only TiO<sub>2</sub> particles can be described with an exponential function (Fig. 2). The number concentration of the TiO<sub>2</sub> particles decreases faster with increasing particle diameter compared to the decrease observed for all particles. This is reflected in the slightly larger (absolute) value of the exponent of the curve fits. We interpret this as an indication that the TiO<sub>2</sub> particles are released from a source with a narrower PSD compared to the overall TSS. ENM, which are tailored for a specific particle size, are expected to have a narrower PSD compared to natural particles and colloids, which are formed by a combination of weathering and precipitation processes.

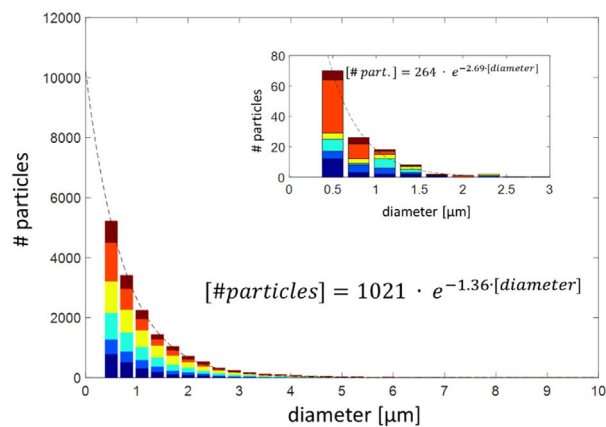


**Fig. 2.** Particle size distribution of all particles detected using automated scanning electron microscopy. TiO<sub>2</sub> particles, identified by a Ti content > 20 wt% are displayed as an inset. Different colors refer to different filters that were investigated. The equations represent best fits to the histogram data.

The sharp decrease observed in the PSD of the TiO<sub>2</sub> particles compared to all particles is thus consistent with an engineered source of the TiO<sub>2</sub> particles. Based on the number and the size of the detected TiO<sub>2</sub> particles and in combination with the filtered volume of the landfill leachate and the scanned area on the filter, the bulk Ti content was calculated from the auto SEM measurements and compared to the results from the ICP-OES measurements (Fig. 3). The Ti concentration calculated from the microscopic analyses (referred to as microscopic Ti) were always within a factor of 6 and mostly within a factor of 3 of the Ti concentrations derived from the ICP-OES (referred to as OES-Ti) measurements. Considering the immense extrapolation involved with the quantification of the microscopic data, this agreement is surprisingly good. The values of the microscopic Ti randomly scatter around the OES-Ti (in 4 measurements, OES-Ti is higher and in two measurements, microscopic Ti is higher) suggesting no systematic over/under-estimation of the Ti concentrations of one method relative to the other. However, the microscopic Ti only includes particles > 500 nm (equivalent projected spherical diameter) with a Ti content > 20% and the OES-Ti includes particle sizes > 200 nm and also Ti from other particles with lower Ti contents (e.g. clay minerals can contain up to a few wt% of Ti). The fairly good agreement between the microscopic-Ti and the OES-Ti thus indicates that the majority of the Ti mass is contained in TiO<sub>2</sub> particles possibly representing white pigments.

One of the key requirements for the quantification of the microscopic data is an even distribution of particles on the filter membrane. To evaluate the variation of the particles distribution on the filter, two filters were measured three times (on different days). Standard deviation derived from these triplicate measurements in the SEM were 19 and 23% and can thus not explain the differences between microscopic - and OES - Ti concentrations. Furthermore, duplicate OES measurements

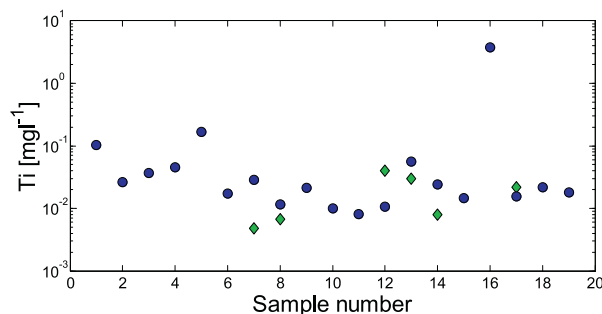


**Fig. 3.** Comparison between the total Ti content derived from ICP-OES measurements (blue dots) and automated scanning electron microscopy analyses (green diamonds).

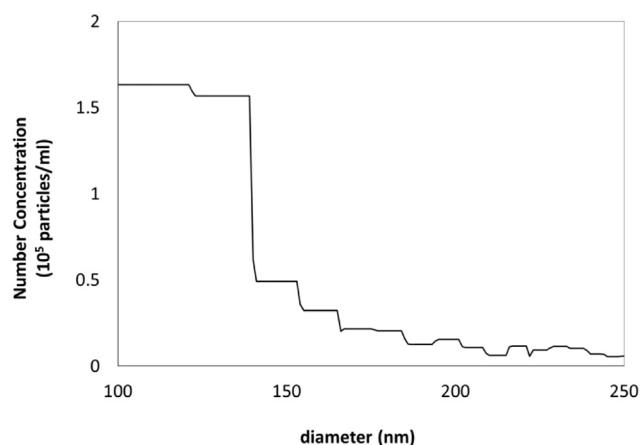


Fig. 4. Particle size distribution of  $\text{TiO}_2$ -particles (all Ti is assumed to be in the form of  $\text{TiO}_2$ ) derived from spICPMS measurements. The lower detection limit for  $\text{TiO}_2$  particles was close to 100 nm. The total number of particles amounted to  $\sim 5 \times 10^5 \text{ mL}^{-1}$ .

from two filters treated the same way also resulted in comparable differences (33%). Therefore, other issues possibly related to sample treatments may explain the observed deviations between calculated microscopic - and OES - Ti concentrations.

### 3.3. Number concentration of Ti-particles in effluent samples

The total number of Ti-particles detected by the spICPMS measurements were  $\sim 5 \times 10^5 \text{ particles mL}^{-1}$ , and the most frequent Ti-containing particles were around 100–150 nm (Fig. 4). Blank corrections were most important for particle sizes close to the size detection limit and contributed to up to two thirds of the recorded signal intensity. With increasing particle diameters, the importance of the blank corrections rapidly decreased and blank corrections only contributed to 5% or less of the recorded signal intensity for particles  $> 170 \text{ nm}$ . The particulate  $\text{TiO}_2$  concentration derived from the spICPMS measurements by integration the PSD and assuming all Ti is in the form of  $\text{TiO}_2$ , amounted to  $\sim 5 \mu\text{g L}^{-1}$ . This value is less by a factor of  $\sim 6$  compared to the total Ti concentrations measured by ICP-OES ( $18 \mu\text{g L}^{-1}$  Ti corresponding to  $30 \mu\text{g L}^{-1} \text{TiO}_2$ ). However, these values should not be compared directly as the samples were treated differently. For spICPMS measurements samples were filtered ( $0.4 \mu\text{m}$ ) and the permeate was investigated and for bulk Ti measurements, samples were filtered ( $0.2 \mu\text{m}$ ) and the retained fraction was analyzed after total digestion. The values therefore are complementary and suggest that a significant fraction of the Ti that would operationally be defined as dissolved was in fact in the form of (nano) particulate Ti-particles.

DLS measurements revealed a moderate increase of the average particle size from  $\sim 240 \text{ nm}$  (before sending the samples to Vienna) to  $\sim 400 \text{ nm}$  (before spICPMS measurements were conducted, time between collecting samples and spICPMS measurements were  $< 36 \text{ h}$  (Table S1)), reflecting the formation of aggregates that occurred during sample transport. As the spICPMS method only records one mass, only the aggregation of two Ti-containing particles would affect the measured mass (and the derived size) and the number concentration of Ti-containing particles. However, due to the low number concentration of Ti-containing particles detected in the landfill leachates, aggregation of two Ti-containing particles is rather unlikely.

### 3.4. Origin of $\text{TiO}_2$ particles in landfill leachates

The PSD extracted from the automatic SEM analyses indicate an exponential increase in particle number with decreasing particle size, but the cutoff of the method is around 500 nm and therefore, the presence of nanoscale  $\text{TiO}_2$  particles in the landfill effluents could not be

confirmed. spICPMS data revealed number concentrations of Ti-particles in the order of  $5 \times 10^5 \text{ particles mL}^{-1}$ , with most particles around 100–150 nm. However, also with spICPMS we were not able to detect  $\text{TiO}_2$  particles  $< 100 \text{ nm}$  as our detection limit was slightly above 100 nm. Although Peters et al. (2014) report slightly lower size detection limits of 50 nm for  $\text{TiO}_2$ , in the presence of elevated Ca concentrations (5–50 mL/L) size detection limits between 75 and 100 nm are reported for spICPMS instruments in reaction mode using ammonia as reaction gas and targeting  $^{48}\text{Ti}$  (Tharaud et al., 2017). These results are very comparable with our size detecting limits of 110 nm and highlight current challenges related to the detection of nanoscale  $\text{TiO}_2$  particles in complex matrices. Furthermore, low Ti concentrations (1–2 wt%) in clay minerals may also have contributed to the particle counts close to the detection limits. Unfortunately, such interferences cannot be avoided using spICPMS, as only one element (more specifically one mass) can be recorded per measurement and reported number concentration of  $\text{TiO}_2$  particles therefore have to be interpreted as maximum values. Recent developments of the spICP - time of flight (TOF) - MS, however, allow the simultaneous detection of multiple elements (Borovinskaya et al., 2013) and Praetorius et al. (2017) successfully distinguished between natural and synthetic Cerium (Ce)-NP based on the characteristic multi elemental composition of the natural and synthetic Ce-NP. A similar approach may also enable distinguishing between Ti-containing clay minerals and pure  $\text{TiO}_2$  particles.

STEM analyses of selected leachate samples showed the presence of individual  $\text{TiO}_2$  particles in the nano-range with a spherical morphology (Fig. 5). These particles are very similar to white pigments detected in façade and urban stormwater runoff (Kaegi et al., 2010). However,  $\text{TiO}_2$  particles (Anatase) of comparable size and morphologies were also observed in soils and were attributed to the dissolution of primary minerals (including Anatase) and precipitation of smaller  $\text{TiO}_2$  particles, also in the form of Anatase. Dissolution of the primary minerals was favored by strong tropical weathering conditions (Cornu et al., 1999). In a temperate climate, however, weathering and formation of Anatase may not be as extensive as in tropical regions and we therefore attribute the  $\text{TiO}_2$  particles observed in the landfill leachate to  $\text{TiO}_2$  white pigments originating from disposed waste of paints and renders. In addition to the identified spherical  $\text{TiO}_2$  particles, angular  $\text{TiO}_2$  particles with a well-defined crystal habitus were observed, suggesting that also natural  $\text{TiO}_2$  particles of comparable sizes are present in the landfill leachates. These particles may originate from soils and sediments excavated at construction sites which is also deposited in the same landfill. Although no quantitative assessment about the abundance of the spherical vs. the angular  $\text{TiO}_2$  particles can be made based on the TEM investigations due to the low abundance of the respective particles in general, the spherical  $\text{TiO}_2$  particles representing most likely white pigments were observed more frequently and are thus assumed to dominate the number of  $\text{TiO}_2$  particles observed in the landfill leachates. The release mechanism of the  $\text{TiO}_2$  particles from the C & D landfill materials is expected to be closely related to the mechanism observed for the release of  $\text{TiO}_2$  particles from façade coatings (Kaegi et al., 2008). When the paint is exposed to ambient conditions, sunshine (UV radiation) and moisture start degrading the (organic) matrix of the paint, leaving a white and chalky powder on the surface of the paint, which is generally referred to as chalking (Khataee et al., 2016; Gaumet et al., 1997; Troutman and Vannoy, 1940). This so-called ‘chalking’ effect has been investigated thoroughly e.g. using microscopic methods such as SEM (Kaempf et al., 1974) or atomic force microscopy (AFM) (Biggs et al., 2001). As a result of chalking, loosely bound particles, such as  $\text{TiO}_2$  pigments contained in the paint are accumulated at the paint surface and can be washed off during rain events either from facade, and possibly also from landfilled construction materials. Crushing of the construction materials during demolition work may additionally break the paints in smaller fragments increasing the available surface for weathering. The degradation of the binder may further be accelerated by photocatalytic reactions caused by nano $\text{TiO}_2$

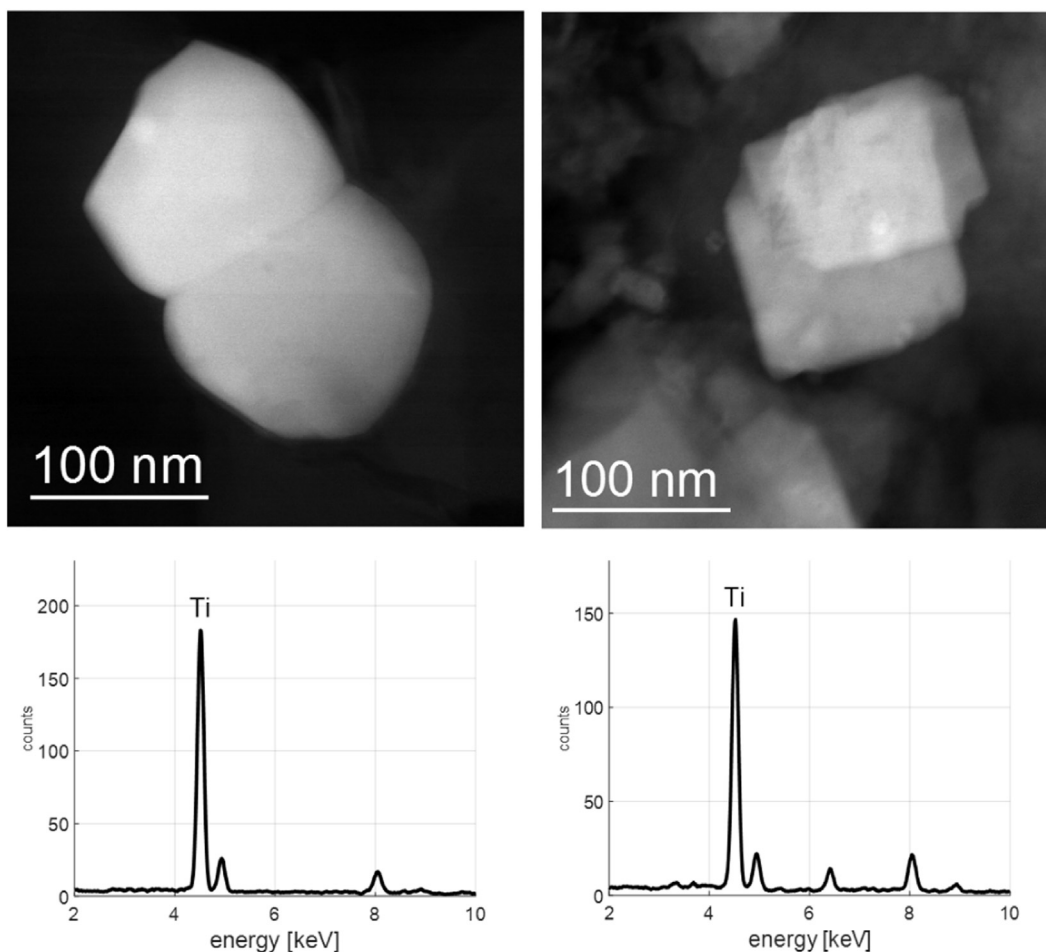


Fig. 5. Typical STEM-HAADF of  $\text{TiO}_2$  particles detected in landfill leachate samples. The particles show a spherical morphology characteristic for white pigments (left). Angular particles suggest a natural origin of the particles (right). Elemental analyses (EDX) confirmed that the particles were  $\text{TiO}_2$  nanoparticles. Although the majority of the  $\text{TiO}_2$  particles detected were above 100 nm, these images revealed that also particle in the nano-range were present in the landfill samples.

used as additives to enhance self-cleaning properties of the paints (Khataee et al., 2016). Thus, it may even be possible that nano- $\text{TiO}_2$  particles from self-cleaning paints eventually being landfilled will be released at a higher rate compared to the  $\text{TiO}_2$  particles used as white pigments. It is possible that organic materials (e.g. humic acid or fulvic acid) in the landfill leachate further facilitated the detachment of  $\text{TiO}_2$  particles from the paint and their transport in the landfill leachate. Based on our dataset, however, we not able to further address the impact of the organic materials on the release of  $\text{TiO}_2$  particles from C & D landfills.

#### 4. Conclusions

The presence of  $\text{TiO}_2$  particles extending into the nano-size range has been observed in leachate samples from a C & D landfill site containing inert waste materials. The total amount of Ti annually discharged from this landfill (8000  $\text{m}^3$  of leachate for 2014) into the surface water was estimated to  $\sim 0.3$  kg corresponding to  $\sim 0.5$  kg of  $\text{TiO}_2$  particles. Automated SEM analyses (particles  $> 500$  nm) suggested that Ti was dominantly present in the form of pure  $\text{TiO}_2$  particles. Results from spICPMS measurements (particles  $< 400$  nm) further indicated a total number concentration of Ti-particles of  $\sim 5 \times 10^5 \text{ mL}^{-1}$ , dominated by particles between 100 and 150 nm. As the spICPMS technique only allows detecting the total mass of Ti per particle, clay minerals containing a few wt% of Ti cannot be distinguished from pure  $\text{TiO}_2$  particles. However, STEM measurements revealed the presence of nanoscale  $\text{TiO}_2$  particles in the leachate

waters, dominantly with a spherical morphology and very similar to white pigments previously reported from stormwater runoff (Kaegi et al., 2008). The use of  $\text{TiO}_2$  particles as proxy for ENM used in C & D materials provides first evidence of the release of ENM from respective landfill sites. Assuming that 1% of white pigments are  $< 100$  nm, about 5 g of nano-scaled  $\text{TiO}_2$  particles were discharged into the aquatic environment from the selected C & D landfill in 2014. However, with the increasing use of tailored nano-paints and -coatings, the amount of released ENM from landfills is expected to increase proportionally. In a next step, specific emission factors for nano- $\text{TiO}_2$  and other ENM predicted at increasing volumes in the construction industry are required to further constrain the extent to which landfills may contribute to the emission of ENM to surface waters.

#### Acknowledgements

The authors acknowledge support of the Scientific Center for Optical and Electron Microscopy ScopeM of the Swiss Federal Institute of Technology ETHZ and of the Electron Microscopy Center at Empa (Swiss Federal Institute for Materials Science and Technology, Dübendorf, Switzerland). The project was funded the Office for Waste, Water, Energy and Air (AWEL) of the Canton Zurich. We thank Christian Sieber (AWEL), Jesper Hansen (AWEL) and the staff from Arge Schwanental for their support. This work was supported by the European Cooperation in the field of Scientific and Technical Research - COST - Action ES1205 (ENTER: The transfer of engineered nanomaterials from wastewater treatment & stormwater to rivers).

## Appendix A. Supplementary data

Supplementary data to this article can be found online at <http://dx.doi.org/10.1016/j.impact.2017.07.004>.

## References

- Al-Kattan, A., Wichser, A., Vonbank, R., Brunner, S., Ulrich, A., Zuind, S., Nowack, B., 2013. *Environ. Sci. Process. Impacts* 15, 2186–2193.
- Al-Kattan, A., Wichser, A., Zuin, S., Arroyo, Y., Golanski, L., Ulrich, A., Nowack, B., 2014. *Environ. Sci. Technol.* 48, 6710–6718.
- Al-Kattan, A., Wichser, A., Vonbank, R., Brunner, S., Ulrich, A., Zuin, S., Arroyo, Y., Golanski, L., Nowack, B., 2015. *Chemosphere* 119, 1314–1321.
- Andresen, L., Christensen, F.M., Nielsen, J.M., 2014. *Nanomaterial in Waste: Issues and New Knowledge*. The Danish Environmental Protection Agency.
- Asmatulu, E., Twomey, J., Overcash, M., 2012. *J. Nanopart. Res.* 14, 1–8.
- Baumann, T., Fruhstorfer, P., Klein, T., Niessner, R., 2006. *Water Res.* 40, 2776–2786.
- Biggs, S., Lukey, C.A., Spinks, G.M., Yau, S.T., 2001. *Prog. Org. Coat.* 42, 49–58.
- Boldrin, A., Hansen, S.F., Baun, A., Hartmann, N.I.B., Astrup, T.F., 2014. *J. Nanopart. Res.* 16, 2394.
- Bolyard, S.C., Reinhart, D.R., Santra, S., 2013. *Environ. Sci. Technol.* 47, 8114–8122.
- Borovinskaya, O., Hattendorf, B., Tanner, M., Gschwind, S., Guenther, D., 2013. *J. Anal. At. Spectrom.* 28, 226–233.
- Bystrzejewska-Piotrowska, G., Golimowski, J., Urban, P.L., 2009. *Waste Manag.* 29, 2587–2595.
- Cornelis, G., 2014. *Nanocount 3.0: Analysing spICP-MS Data in Style*.
- Cornu, S., Lucas, Y., Lebon, E., Ambrosi, J.P., Luizao, F., Rouiller, J., Bonnay, M., Neal, C., 1999. *Geoderma* 91, 281–295.
- Deer, W.A., Howie, R.A., Zussman, J., 1992. *An Introduction to the Rock-forming Minerals*. Wiley, New York.
- Der Schweizerische Bundesrat, 2011.**
- Dulger, M., Sakallioğlu, T., Temizel, I., Demirel, B., Cöpy, N.K., Onay, T.T., Uygüner-Demirel, C.S., Karanfil, T., 2016. *Chemosphere* 144, 1567–1572.
- Gaumet, S., Siampiringue, N., Lemaire, J., Pacaud, B., 1997. *Surf. Coat. Int.* 80, 367–372.
- Gondikas, A.P., von der Kammer, F., Reed, R.B., Wagner, S., Ranville, J.F., Hofmann, T., 2014. *Environ. Sci. Technol.* 48, 5415–5422.
- Gottschalk, F., Sonderer, T., Scholz, R.W., Nowack, B., 2009. *Environ. Sci. Technol.* 43, 9216–9222.
- Gounaris, V., Anderson, P., Holsen, T., 1993. *Environ. Sci. Technol.* 27, 1381–1387.
- Hempelmann, U., Buxbaum, G., Völz, H.G., 2005. *Industrial Inorganic Pigments*. Wiley-VCH Verlag GmbH & Co. KGaA.
- Hennebert, P., Avellan, A., Yan, J., Aguerre-Chariol, O., 2013. *Waste Manag.* 33, 1870–1881.
- Hincapié, I., Caballero-Guzman, A., Hiltbrunner, D., Nowack, B., 2015. *Waste Manag.* 43, 398–406.
- Hischier, R., Nowack, B., Gottschalk, F., Hincapie, I., Steinfeldt, M., Som, C., 2015. *J. Nanopart. Res.* 17, 68.
- Jensen, D.L., Christensen, T.H., 1999. *Water Res.* 33, 2139–2147.
- Kaegi, R., Ulrich, A., Sinnet, B., Vonbank, R., Wichser, A., Zuleeg, S., Simmler, H., Brunner, S., Vonmont, H., Burkhardt, M., Boller, M., 2008. *Environ. Pollut.* 156, 233–239.
- Kaegi, R., Sinnet, B., Zuleeg, S., Hagendorfer, H., Mueller, E., Vonbank, R., Boller, M., Burkhardt, M., 2010. *Environ. Pollut.* 158, 2900–2905.
- Kaempf, G., Papenrot, W., Holm, R., 1974. *J. Paint Technol.* 46, 56–63.
- Keller, A.A., McFerran, S., Lazareva, A., Suh, S., 2013. *J. Nanoparticle Res.* 15, 1692.
- Khan, I.A., Berge, N.D., Sabo-Attwood, T., Ferguson, P.L., Saleh, N.B., 2013. *Environ. Sci. Technol.* 47, 8425–8433.
- Khataee, A., Moradkhannejhad, L., Heydari, V., Vahid, B., Joo, S.W., 2016. *Pigm. Resin Technol.* 45, 24–29.
- Lozano, P., Berge, N.D., 2012. *Waste Manag.* 32, 1699–1711.
- Marcoux, M.-A., Matias, M., Olivier, F., Keck, G., 2013. *Waste Manag.* 33, 2147–2156.
- Matura, M., Ettler, V., Jezek, J., Mihaljevic, M., Sebek, O., Sykora, V., Klementova, M., 2010. *J. Hazard. Mater.* 183, 541–548.
- Matura, M., Ettler, V., Klementova, M., 2012. *Waste Manag. Res.* 30, 530–541.
- Mavrocordatos, D., Perret, D., 1995. *Commun. Soil Sci. Plant Anal.* 26, 2593–2602.
- Mitrano, D.M., Motellier, S., Clavaguera, S., Nowack, B., 2015. *Environ. Int.* 77, 132–147.
- Mitrano, D.M., Mehrabi, K., Dasilva, Y.A.R., Nowack, B., 2017. *Environ. Sci. Nano* 4, 480–492.
- Mueller, N.C., Buha, J., Wang, J., Ulrich, A., Nowack, B., 2013. *Environ. Sci. Process. Impacts* 15, 251–259.
- Olabarrieta, J., Zorita, S., Pena, I., Rioja, N., Monzon, O., Benguria, P., Scifo, L., 2012. *Appl. Catal. B Environ.* 123, 182–192.
- Peters, R.J.B., Rivera, Z.H., van Bommel, G., Marvin, H.J.P., Weigel, S., Bouwmeester, H., 2014. *Anal. Bioanal. Chem.* 406, 3875–3885.
- Praetorius, A., Gundlach-Graham, A., Goldberg, E., Fabienke, W., Navratilova, J., Gondikas, A., Kaegi, R., Gunther, D., Hofmann, T., von der Kammer, F., 2017. *Environ. Sci. Nano* 4, 307–314.
- Reinhart, D.R., Berge, N.D., Santra, S., Bolyard, S.C., 2010. *Waste Manag.* 30, 2020–2021.
- Sun, T.Y., Gottschalk, F., Hungerbühler, K., Nowack, B., 2014. *Environ. Pollut.* 185, 69–76.
- Tharaud, M., Gondikas, A.P., Benedetti, M.F., von der Kammer, F., Hofmann, T., Cornelis, G., 2017. *J. Anal. At. Spectrom.* 32, 1400–1411.
- Troutman, R.E., Vannoy, W.G., 1940. *Ind. Eng. Chem.* 32, 232–237.
- van Broekhuizen, F.A., van Broekhuizen, P.C., 2009. *Nanotechnology in the European Construction Industry-State of the Art 2009*. IVAM UvA BV, Amsterdam-NL.
- van Broekhuizen, P., van Broekhuizen, F., Cornelissen, R., Reijnders, L., 2011. *J. Nanopart. Res.* 13, 447–462.
- Weir, A., Westerhoff, P., Fabricius, L., Hristovski, K., von Goetz, N., 2012. *Environ. Sci. Technol.* 46, 2242–2250.
- Zuin, S., Gaiani, M., Ferrari, A., Golanski, L., 2013. *J. Nanopart. Res.* 16 (UNSP 2185).
- Zuin, S., Massari, A., Ferrari, A., Golanski, L., 2014. *Sci. Total Environ.* 476, 298–307.